N-Substituted Azacalixphyrins: Synthesis, Properties, and Self-Assembly

Zhongrui Chen, Rose Haddoub, Jerome Mahe, Gabriel Marchand, Denis Jacquemin, Judicaelle Andeme Edzang, Gabriel Canard, Daniel Ferry, O. Grauby, Alain Ranguis, et al.

N-substituted Azacalixphyrins: synthesis, properties and self-assembly

Zhongrui Chen,[a] Rose Haddoub,[a] Jérôme Mahé,[b] Gabriel Marchand,[b] Denis Jacquemin,* [b,c] Judicaelle Andeme Edzang,[a] Gabriel Canard,[a] Daniel Ferry,[a] Olivier Grauby,[a] Alain Ranguis,[a] and Olivier Siri*[a]

[a] Aix Marseille Université, CNRS UMR 7325, *Centre Interdisciplinaire de Nanosciences de Marseille* (CINaM), 13288 Marseille, France
Fax: (+33) 491 41 8916, E-mail: olivier.siri@univ-amu.fr

[b] CEISAM UMR CNRS 6230, Université de Nantes, 2 rue de la Houssinière, BP 92208, 44322 Nantes Cedex 3, France. E-mail: Denis.Jacquemin@univ-nantes.fr

[c] Institut Universitaire de France, 103 blvd St Michel, 75005 Paris Cedex 05, France

Supporting information for this article is given via a link at the end of the document.

Dedicated to Professor Reinhard Neier on the occasion of his retirement

Abstract: *Pre- and post-introduction of substituents with respect to the macrocyclization step leads to previously unknown N-substituted azacalixphyrins. The stepwise synthesis approach has been studied in details highlighting the key role of the N-substituents of the precursors and/or the intermediates in terms of reactivity. Based on a combined experimental and theoretical investigation, the relationship between the properties of the macrocycles and their degree of substitution is rationalized. Depending on the nature of the N-substituents, the formation of supramolecular ribbon-like structures could also be observed, an outcome demonstrated by combined TEM, SEM, AFM and FTIR experiments*.

Introduction

Azacalixphyrin **1** is the first member of an emerging class of azamacrocycles that recently appeared in the literature[1] and revealed unusual properties, e.g., a unique electronic distribution (biszwitterionic character), an absorption spectrum covering the whole visible region with intense absorption bands up to 879 nm, and a very stable dianionic aromatic ring. Importantly, this molecule belongs to porphyrinoids and can be viewed as the first "pyrrol-free" aza-analogue of porphyrazine derivatives **2a** (including phthalocyanines and related macrocycles bearing *meta*-phenylene subunits),[2] and porphyrins **2b**[3] which are the most adaptable macrocycles with applications covering the whole spectrum of science. The exceptional versatility of porphyrins can be explained by their peculiar electronic and structural features, but also by their synthetic accessibility which allows the introduction of tunable substituents at will.[4-9] By analogy, the newly designed azacalixphyrin **1** appears to be the prime member of a family of extremely promising but yet almost completely unexplored macrocycles.[1] It is noteworthy that **1** – lacking substituents - suffers from a very low solubility which impedes straightforward experimental studies. This limitation parallels the case of porphine in the history of the porphyrins[10,11] and underlines the interest of developing access to substituted azacalixphyrins **3**, subsequently paving the way to applications in several major sectors.[12] In this context, the presence of peripheral nitrogen atoms on **1** should allow the possible introduction of structural diversity which, in turn, can impact the physicochemical properties of the macrocycle and its behaviors (solubility, geometry, self-assembly).

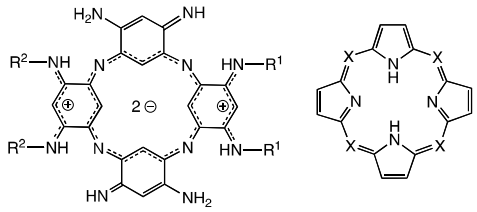

1 $R^1 = R^2 = H$
3 $R^1 =$ or $\neq R^2 =$ alkyl

2a X = N
2b X = C-R

Herein, we describe the stepwise synthesis of unprecedented N-substituted derivatives **3**. Two different approaches based on pre- and post-introduction of substituents were developed and the reactivity of the intermediates is discussed in detail in order to scrutinize the key role of the substituents. Spectrophotometrical and theoretical studies were also performed to obtain first insights into the structure-properties relationships for these new entities. In addition, improving the solubility allowed the access to a new class of nanoribbons with mechanical properties which might be of major interest in a broad range of applications ranging from opto-electronic and energy to surface science and medicine.[13]

Results and Discussion

Synthesis and characterization

A first synthetic approach to prepare N-substituted analogues consists in the direct introduction of substituents on the azacalix[4]arene **4** (post-introduction with regard to the macrocyclization step, see Scheme 1) due to presence of four external amine functions that could be potentially substituted. To this end, molecule **4** – prepared in one step by nucleophilic aromatic substitution (S_NAr)[1] - was reacted with butyryl chloride in MeCN to afford the corresponding tetraamido-azacalixarene **5** in 55% yield (Scheme 1, route 1).[14] Unfortunately, the reduction of the carbonyl functions in **5** with $LiAlH_4$ did not lead to the expected N-substituted analogue **6b** owing to side reactions involving the acidic NH protons of the bridges (deprotonation in presence of hydride). An alternative route was then envisaged by the direct reductive amination of **4** (Scheme 1, route 2). This latter was thus reacted with *i*-butyraldehyde in acidified DMF or THF to afford intermediate **A** (not isolated) which was directly reduced by sodium cyanoborohydride in **6a** in approx. 40% yield (Scheme 1). We underline that the use of *n*-butyraldehyde vice *i*-butyraldehyde did not give - under similar conditions - the expected compound **6b** but instead penta- and hexa-alkylated derivatives. The NO_2 reduction of **6a** by hydrazine ($N_2H_4{\cdot}H_2O$) with Pd in THF gave the electron-rich intermediate **B** (highly unstable) which was oxidized under air into the target N-substituted azacalixphyrin **3a** as a green solid in 62% yield (Scheme 1).

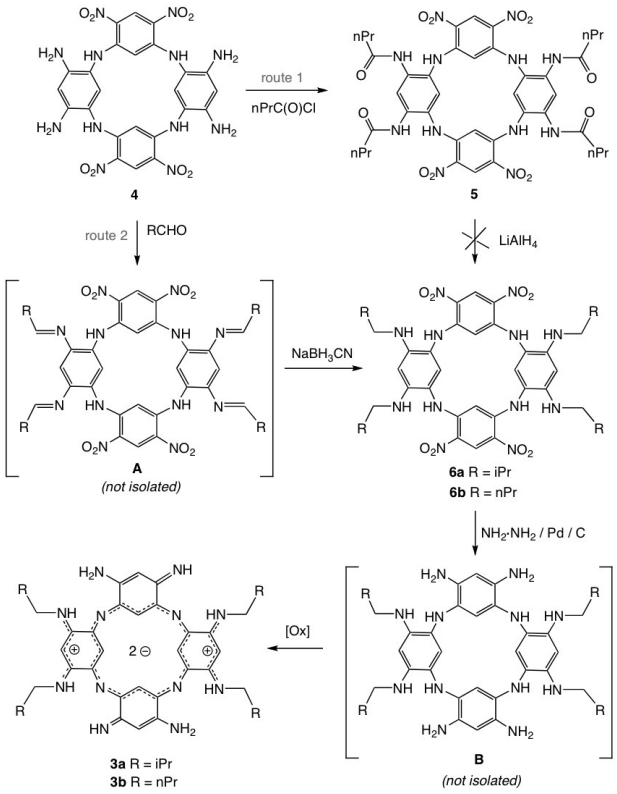

Scheme 1. Synthesis of N-substituted azacalixphyrin **3a**.

The reductive amination of **4** being poorly reproducible and strongly limited (**6b** could not be accessible *via* this route), we decided to develop a more versatile and efficient approach based on the introduction of N-substituents prior to the macrocyclization step. This approach required the synthesis of the N-substituted tetraaminobenzene derivatives **8a**[15] and **8b** (see Scheme 2 and the SI), for which two NH_2 functions in *meta* position are available as nucleophilic partners in S_NAr reactions (Scheme 2).[16,17] We underline that the presence of additional N-Boc substituents in **8a** and **8b** prevents their oxidation by air. The condensation reaction between **8a** and the electron deficient aryl **7** (1 equiv.) in refluxing MeCN for 3 hours led to a mixture of the [1+1] and the [1+2] adducts (**9a** and **10a**) in 18% and 12% yield, respectively (Scheme 2). The same reaction conducted for 3 days with 2 equiv. of **7** produces the exclusive formation of the [2+1] product **10a** in 28% yield (Scheme 2). When the reaction time was extended to 10 days, the yield of **10a** jumped to 86% with no occurrence of **9a**. The ^1H NMR spectrum of **10a** shows the NH resonance at 10.02 ppm suggesting the presence of intramolecular NH···O_2N hydrogen bonding interactions that restrict the rotation and subsequently leads to a conformation of the backbone of the uncyclic intermediate favorable for the cyclization step. The macrocyclization from the reaction between **10a** or **8a** in refluxing MeCN provided the BOC protected macrocycle **11a** as a red solid in 31% yield after column chromatography (Scheme 2). When precursor **8b** was used instead of **8a** as nucleophilic partner, its stoechiometric condensation with **7** in presence of N(*i*Pr)$_2$Et yielded neither **9b** nor **10b**. The reaction finally succeeded in THF with 2,4,6-collidine as base

affording **9b** and **10b** in 18% and 12% yields, respectively (Scheme 2). However, the macrocyclization from **10b** or **8b** failed in refluxing MeCN indicating the crucial role of the length of the N-alkyl substituents (C_4 vs C_8) on the reactivity of the [1+2] adducts.

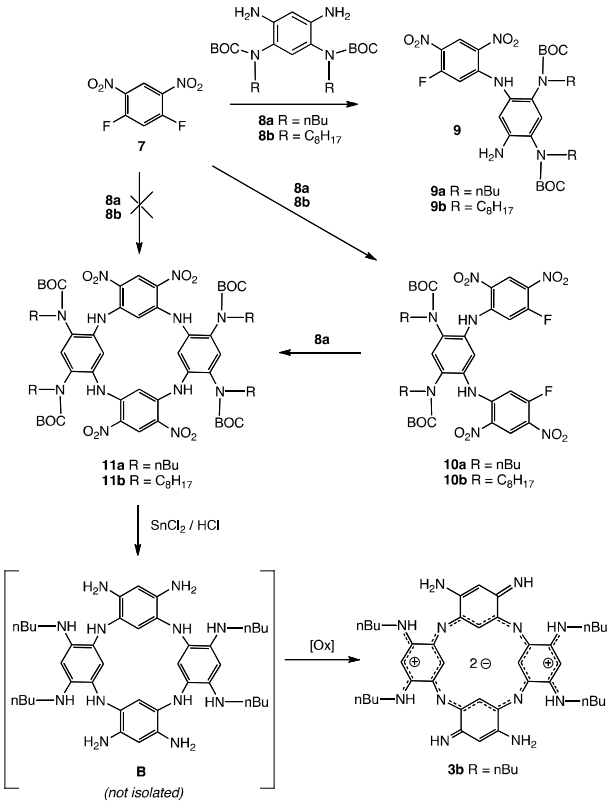

Scheme 2. Synthesis of the N-substituted azacalixphyrin **3b**.

It is noteworthy that macrocycle **11a** could not be formed directly from a stoichiometric condensation between **7** and **8a** most probably owing to the major formation of **9a** that cannot react on itself to form **11a**, and/or the limited reactivity of **8a** under these conditions.

The reduction of **11a** by $SnCl_2$ in refluxing EtOH led to the formation of the electron-rich macrocycle intermediate **B** which after air-oxidation and rearrangement gave the bis-zwitterionic azacalixphyrin **3b** as a green solid in 59% yield. In order to further extend this class of tetraazamacrocycles, analogues with lower symmetry were next synthesized. To this end, azacalixarene **6c** and **6d** were prepared in two steps by S_NAr (Scheme 3). The nucleophilic partners **12a** and **12b** – that could be isolated in acidic medium with no need of BOC protective groups - were first reacted with **7** (2 equiv.) in the presence of N(*i*Pr)$_2$Et at 0°C to afford the [2+1] adducts **13a** and **13b** in 54 % and 67 % yield, respectively.

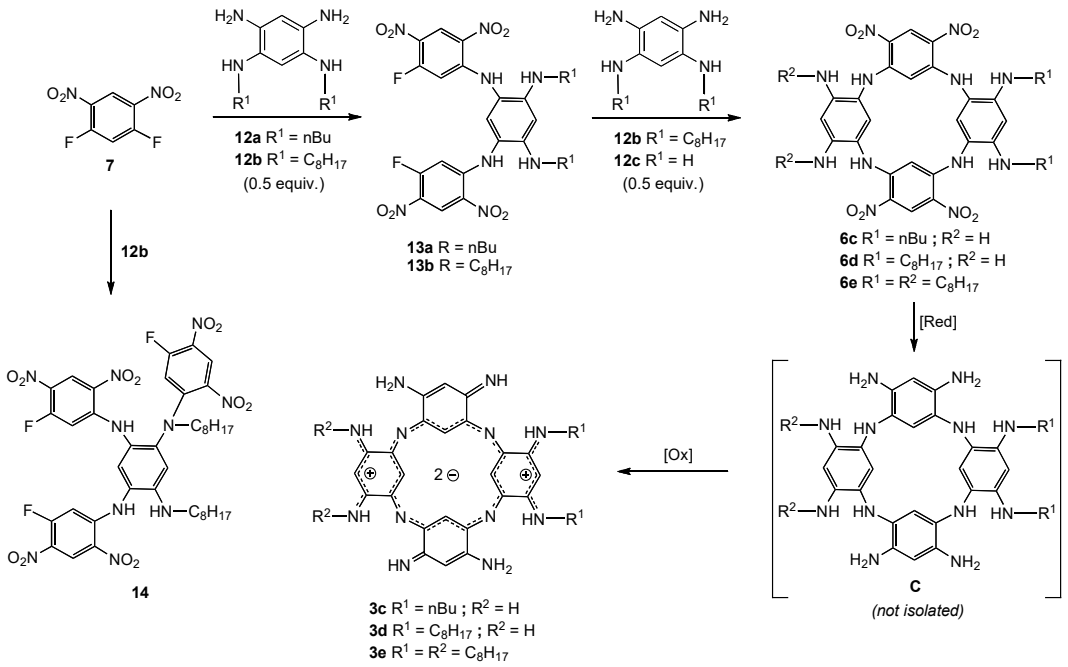

Scheme 3. Synthesis of N-substituted azacalixphyrin **3c-e**.

It is noteworthy that a tetraaryl compound **14** could be obtained as well in 12% yield from **12a** in excess (2.2 equiv). Compounds **14** and **13b** were fully characterized including by X-ray analysis (Figures. 1 and 2, respectively). The structure of the former revealed the tertiarization of one of the nitrogen atoms and the vicinity of the F(1) and F(2) fluorine atoms (d[F(1)-F(2)] = 6.058 Å) induced by the presence of non-bonding interactions (Figure 1).

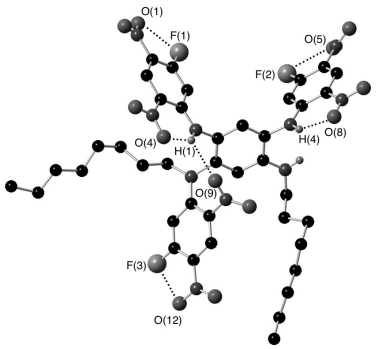

Figure 1. X-ray structure of **14** .

As can be seen in Figure 1, molecule **14** presents a conformation favorable for the cyclization step despite the steric hinderance. This observation contrasts with the X-ray diffraction study on single crystal of **13b** that shows an estrangement between the two fluorine atoms (d[F(3)-F(4)] = 11.146 Å) probably due to the presence of the N-H···F hydrogen bonding interactions (Figure 2).

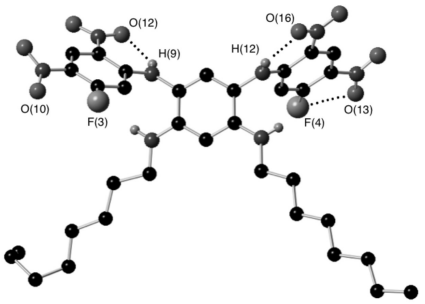

Figure 2. X-ray structure of **13b**.

Although the geometry of **13b** in the solid-state looks not favorable for macrocyclization reaction, their reaction with 1,2,4,5-tetraaminobenzene **12c** in refluxing MeCN provided azacalixarenes **6d** in 83% as a pure orange solid by simple filtration (no need of column chromatography) (Scheme 3). Similarly, macrocycle **6c** could be obtained from **13a** in 70% yield. This observation suggested that the solid-state geometry of **13b** is not retained in solution and can evolve into more favorable conformations for the cyclization step. Indeed, theoretical investigations located several nearly iso-energetic minima with vastly different F-F distances (see Figure 3). These DFT calculations also reveal small barriers for the rotations of the phenyl rings that can be overcome in refluxing MeCN.

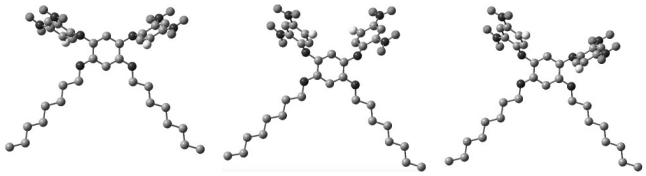

Figure 3. Representation of three conformers of **13b** as identified by DFT [PBE0/6-31G(d)] calculations. The relative free energies of the three conformers are 1.0, 0.0 and 0.5 kcal/mol (from left to right), whereas the F-F distances are 11.2, 9.2 and 6.0 Å, respectively.

Finally, the NO_2 reduction of **6c-e** gave the corresponding octaaminoazacalix[4]arenes **C** which underwent an aerobic oxidation to afford the target macrocycles **3c**, **3d** and **3e** as green solids in 83%, 55% and 89% yield, respectively. Note that this stepwise approach - involving the unprotected precusors **12b** and **13b** (as opposed to **8b** and **10b**) - allowed also the isolation of the tetraoctylated azacalixarene **6e** as precusor of **3e** (Scheme 3). As expected, N-substituted azacalixphyrins **3a**-**3e** appear much more soluble than their unsubstituted parent **1**. For instance, the solubility in MeOH at room temperature increases with the number of N-alkyl substituents following: s = 0.015, 4 and 11 g/L for **1**, **3c** and **3b**, respectively. In addition, molecule **3a** is also much more soluble than its isomer **3b (**s = 32 *vs* 11 g/L) most likely due to the presence of branched chains impeding strong van der Walls interactions.

Absorption Spectroscopy

The absorption spectra of azacalixphyrins in MeOH have essentially the same features compared to **1**,[1] exhibiting four main bands covering the entire visible light spectrum and an additional broad and intense absorption in the NIR region (see Figure 4 for three illustrative species). These absorption profiles are consistent with diprotonated species **3a**-**e**·**2H**$^+$ resulting from acid-base reaction of **3a**-**e** with water molecules present in methanol (azacalixphyrins are very strong bases).[18] Interestingly, the low energy transition is slightly redshifted when the number of alkyl groups increases, going from the unsubstituted parent **1**·**2H**$^+$ (λ_{max} = 879 nm),[1] to the dialkylated molecule **3c**·**2H**$^+$ (λ_{max} = 885 nm) and finally to the tetraalkylated azacalixphyrin **3b**·**2H**$^+$ (λ_{max} = 890 nm) (see Figure 4).

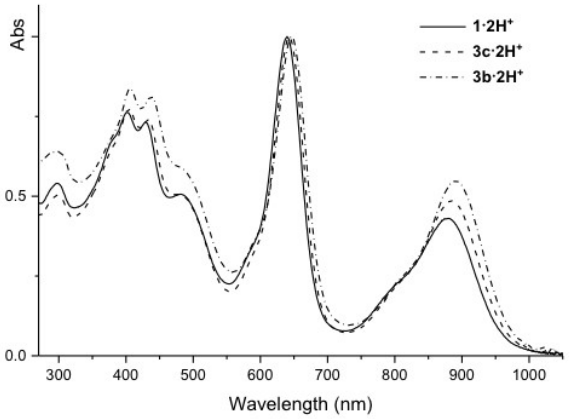

Figure 4. Normalized absorption spectra of **1·2H$^+$**, **3c·2H$^+$**, and **3b·2H$^+$** in MeOH.

NMR Spectroscopy

^{1}H NMR spectra of azacalixphyrins **3a-e·2H$^+$** in DMSO showed downfield signals (-2 < δ < -4 ppm) for the internal C-H protons in agreement with the aromatic character of this family of tetraazamacrocycles (see also theoretical simulations).[1a] Azacalixphyrin **3b·2H$^+$** (see below) was used as a model compound for a temperature-dependent ^{1}H NMR analysis because of its good solubility in MeOH.

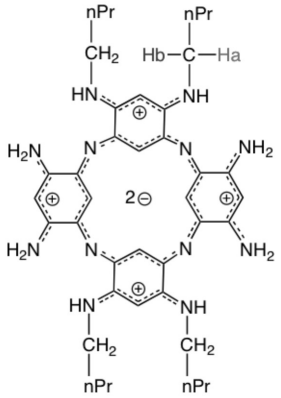

The spectrum of **3b·2H$^+$** at room temperature (290 K) shows seven signals, indicating an average structure in solution (Figure 5). When the temperature is decreased from 290 to 180 K, the most striking feature of this spectrum is the modification observed for the internal CH and the N-CH_2 methylenic protons. The internal CH protons which appeared at room temperature in an upfield region at δ = -4.0 ppm (stronger aromaticity of **3b** compared to the parent **1** for which δ = -2.1 ppm) as a broad signal, diverges at 260 K into two peaks at -4.15 and -4.96 ppm as expected for the C_{2v} point-group symmetry of **3b·2H$^+$**. Simultaneously, the signal of the methylenic protons - which appeared as a singlet at δ = 3.75 ppm - is split into two singlets at 3.77 and 3.96 ppm (Figure 5).

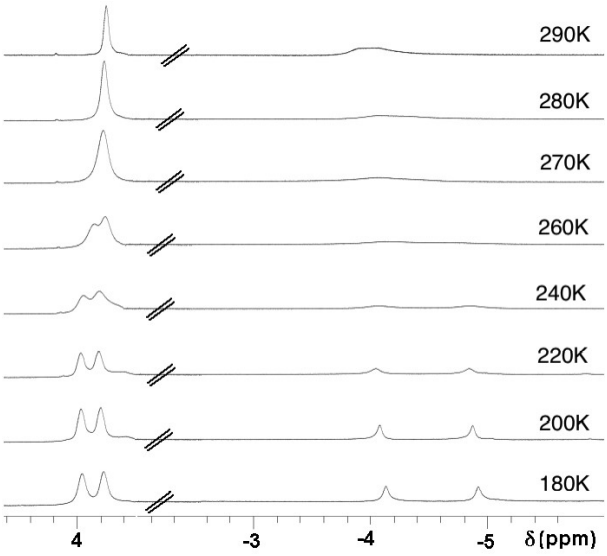

Figure 5. Temperature-dependent ^{1}H NMR spectra of **3b·2H$^+$** in MeOD-d_4.

These observations suggest that different conformers of **3b·2H$^+$** in equilibrium coexist above 260K (signal averaging) whereas a single one with 1,3-alternate conformation is observed below this temperature (C_{2v} symmetry). The presence of two different magnetic environments for the diastereotopic N-CH_2 protons (Ha and Hb) can then be interpreted as a result of a freeze that restricted the rotation process of the substituents at low temperature.

Theoretical Calculations

DFT calculations have been carried out on the protonated forms of three relevant systems, **1·2H$^+$**, **3b·2H$^+$** and **3c·2H$^+$** (see Experimental Section for details), to shed light onto their structure and electronic properties. The interested reader may find a detailed investigation of the neutral **3b** in the SI. First, several conformations for the side alkyl chains have been tested, but the most stable conformers present the four alkyl chains symmetrically arranged around the core and extending from the core towards the exterior (Figure 6). In other words, coiled conformations for the side butyl chains are not favored.

Secondly, we have computed the Nucleus-Independent Chemical Shift (NICS, see the Experimental Section) of the central macrocycle and six-member rings in order to quantify the aromaticity of the system. The macrocycles of **3b·2H$^+$** and **3c·2H$^+$** are found to be strongly aromatic (-8.7 ppm and -8.5 ppm, comparable to benzene), which is consistent with the experimental NMR spectrum showing the internal proton strongly upfield. For comparison **1·2H$^+$** presents a NICS of -8.6 ppm, indicating that alkyl substituents very slightly increase aromaticity (**3b·2H$^+$**), whereas asymmetry is slightly detrimental (**3c·2H$^+$**), as expected. In contrast, all phenyl rings are anti-aromatic. In **1·2H$^+$**, the NICS is +5.7 ppm for all four sub-cycles, whereas in **3b·2H$^+$**, the NICS indicates a more anti-aromatic character for the two six-member cycles bearing the butyl chains (+6.0 ppm) than for two others (+5.3 ppm). The same holds in **3c·2H$^+$** with the NICS at the center of the phenyl ring bearing the butyl reaching +6.7 ppm, whereas the other cycles have a NICS of +5.5 ppm.

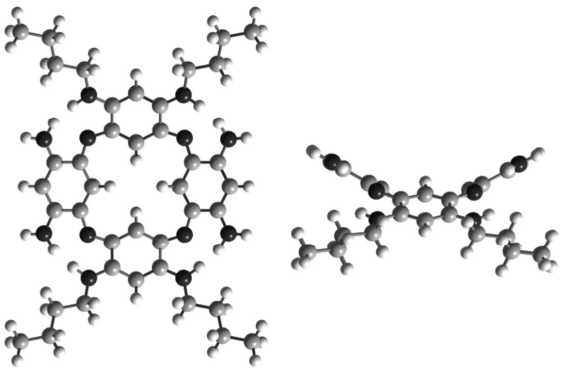

Figure 6. Side and top views of the most stable conformation for the side butyl chains in **3b·2H$^+$** determined by DFT.

Thirdly, we have determined the transition energies of the three structures with Time-Dependent Density Functional Theory (TD-DFT). In **1·2H$^+$** (D_{2d} point group) the longest wavelength transition (calculated at 780 nm, measured at 879 nm, a 0.18 eV error, in the expected range at this level of theory) corresponds to two degenerate *E* state for a total oscillator strength, *f*, of 0.12, whereas

the second experimental band (at ca. 650 nm, see Figure 4) is attributed to two other degenerate *E* states computed at 594 nm (total *f* = 0.76). In **3b·2H$^+$** (C_{2v} point group), the degeneracy is formally lifted but the two first excited-states of B_2 and B_1 symmetry remain quasi-degenerate and they correspond to a λ_{max} of 784 nm (total *f* = 0.19), slightly redshifted compared to **1**, consistently with experiment. These low-lying singlet states can be mainly ascribed to transitions from the HOMO-1 and HOMO to the LUMO and LUMO+1. These orbitals are represented in Figure 7 and are, as expected, of π and $\pi*$ characters with no direct contribution from the alkyl chains, explaining their moderate impact on the optical spectra. In line with experiment, the λ_{max} determined for the C_s **3c·2H$^+$**, 783 nm (*f* = 0.15), is in between the values determined for **1·2H$^+$** and **3b·2H$^+$**.

Eventually, we have compared the relative stabilities and the properties of the possible tautomers of (the neutral) **1** and **3b**, and we found that the tautomeric blend is affected by the presence of substituents (see the SI for details).

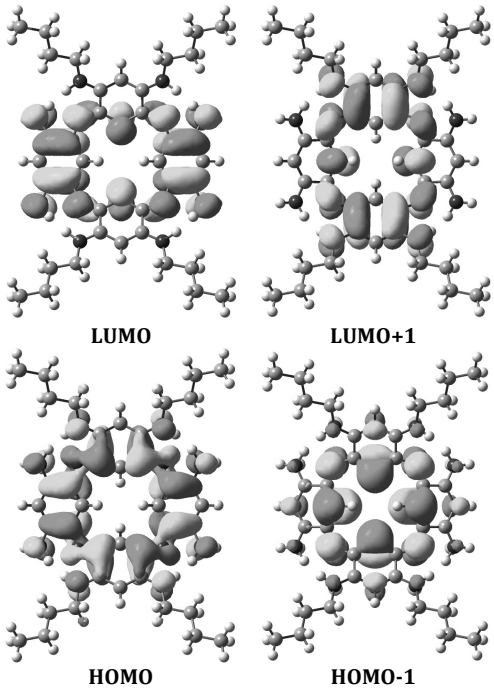

Figure 7. Frontier molecular orbitals of **3b·2H$^+$**.

Electrochemical studies

The electronic properties of **3a-e** were also examined by cyclic voltammetry (CV) at 1.10^{-3} M in DMF (Table 1). There is clearly no obvious impact of the peripheral alkyl substituents on the redox properties of **3a-e** featuring half-wave oxydation and reduction potentials that are very close to the ones of the parent compound **1** (-0.5 V and 0.5 V *vs* SCE). This observation confirms the absence of significant electronic effects arising from the N-substituents as seen previously in the frontier molecular orbitals.

Table 1. Redox properties of N-substituted azacalixphyrins (vs SCE)

Compound	$E_{1/2}$ (reduction) (V)	$E_{1/2}$ (oxidation) (V)
1	-0.51	0.44
3b	-0.48	0.46
3c	-0.48	0.50
3d	-0.51	0.44
3e	-0.50	0.44

Self-assembly

Unlike all the other azacalixphyrins, **3e·2H$^+$** appeared able to self-assemble in MeOH into well-defined molecular ribbons that are as long as 1.0 to 1.6 mm (Figure 8).

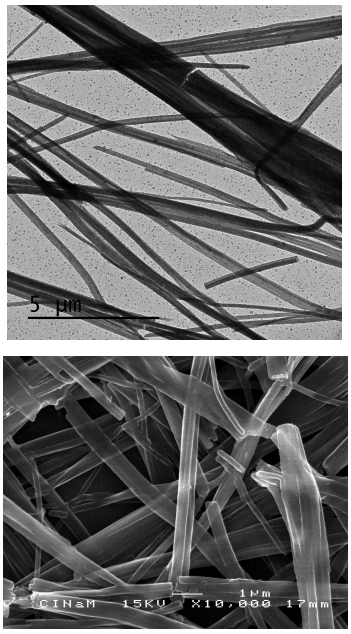

Figure 8. TEM (top), SEM (bottom) images of self-assembled **3e·2H$^+$**.

Such a behavior highlights the crucial role of the N-substituted alkyl length (C_8 in **3e** *versus* C_4 in 3**b**) on the formation of the supramolecular network. Investigations of **3e·2H$^+$** by transmission and scanning electron microscopy (TEM and SEM, respectively) revealed the formation of ~700 nm wide ribbon-like structures (Figure 8). Images obtained by Atomic Force Microscopy (AFM) on freshly cleaved Mica disc confirmed the width and showed a thickness of ~ 200 nm (Figure 9).

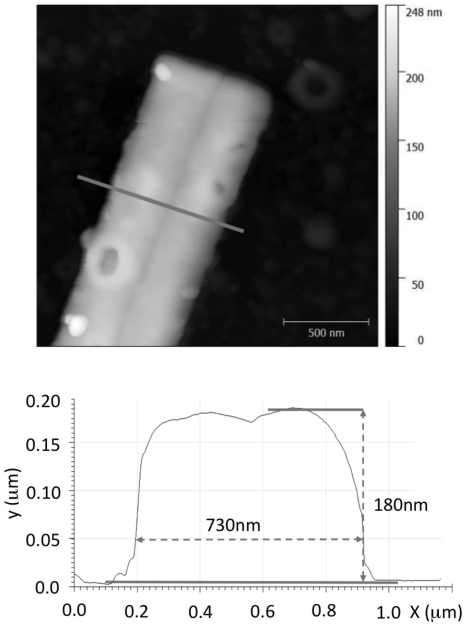

Figure 9. AFM image (top) and profile analysis (bottom) of self-assembled **3e·2H$^+$**.

Transmission Electron Microscopy experiments further demonstrate the mechanical properties of the ribbon. More specifically, Figure 10 shows different views depending on the angle which clearly reveal a flexibility of the ribbon.

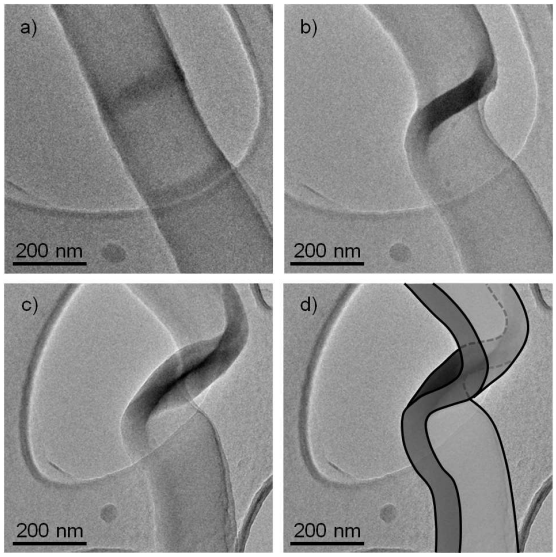

Figure 10. TEM images of **3e·2H$^+$** ribbon observed at respective tilt angles of a) 0 deg, b) 30 deg and c) 60 deg. A scheme of the fiber showing its curvature is represented in d) for a tilt angle of 60 deg.

FTIR spectra of **3e·2H$^+$** as powder or nanoribbon were similar and showed absorbances centered at 3300 cm^{-1} that can be assigned to the stretching vibration of the -NH_2^+ groups (Figure 11).[19] The presence of additional bands at ~3450 and ~1150 cm^{-1} for the ribbon might be due to the vibration of OH^- (acting as counter anions of the diprotonated species) and the C-H vibration of the alkyl chains involved in the van der Waals interactions,[20] respectively.

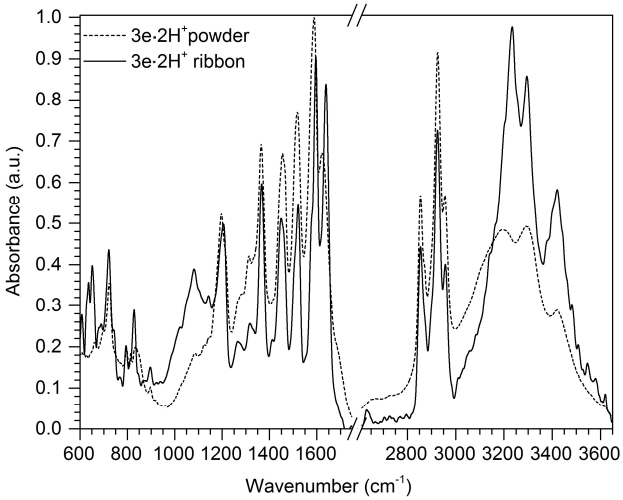

Figure 11. FT-IR spectra of **3e·2H$^+$**.

The absence of intense bands at ~1200 cm^{-1} (C-O vibration) is consistent with the absence of MeOH molecules in the ribbon suggesting a self-assembly based exclusively on intermolecular interactions between azacalixphyrin units. The formation of nanoribbons based on **3e·2H$^+$** is thus probably controlled by electrostatic, H-bonding and π–π intermolecular interactions but also, and importantly, by van der Waals interactions between the octyl chains. DFT calculations on **3e·2H$^+$** revealed indeed a 1,3-alternate conformation in which the four C_8 substituents are located in the same side of the molecule favoring probably a « zig-zag » arrangement in the solid-state as depicted in Figure 12.

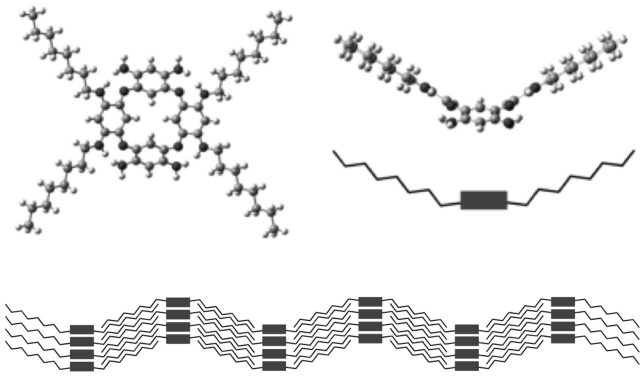

Figure 12. DFT optimized structure of **3e·2H$^+$** (top) and its model of self-assembly (bottom)

Conclusion

In summary, we have disclosed two different synthetic routes to obtain N-substituted azacalixphyrins, the first substituted members of these new macrocycles. The pre-introduction approach appears much more versatile and efficient than the post-introduction. This stepwise synthetis revealed the influence of the N-substituents on the reactivity of the intermediates. Based on combined theoretical and experimental studies, the relationship between the properties of the macrocycle and their degree of substitution is rationalized. Although the presence of N-substituents at the periphery induces small changes in the optical spectrum and redox behavior, the possibility to fine-tune the nature and the number of substituents impact the physicochemical properties of the macrocycle such as the solubility. By increasing the solubility properties of the azacalixphyrins, we demonstrated that this new family of macrocycles can enter in the field of materials science as shown by the formation of well-defined molecular ribbons based on **3e·2H$^+$**. Thus, the access to tunable N-substituted azacalixphyrins becomes now possible and paves the way for a wide range of applications ranging from supramolecular chemistry (as building block) and energy (DSSC solar cell) to coodination chemistry (as ligand) and photonic (as NIR dyes).

Experimental Section

General Remarks: All reagents were used as received. ^{1}H Nuclear Magnetic Resonance (NMR) spectra were recorded on a Bruker Avance 250 Ultrashield or on a Bruker Avance 500 Ultrashield or on a JEOL ECS400 NMR spectrometer Chemical shifts are reported in delta (δ) units, expressed in parts per million using the residual protonated solvent as an internal standard (For proton: $CDCl_3$, 7.26 ppm; MeOD-d_4, 3.31 ppm; DMF-d_7, 2.75 ppm; DMSO-d_6, 2.50 ppm; Acetone-d_6, 2.05 ppm; THF-d_8, 1.72 ppm. For ^{13}C: $CDCl_3$, 77.0 ppm; MeOD-d_4, 49.1 ppm; DMSO-d_6, 39.4 ppm; Acetone-d_6, 30.8 ppm; THF-d_8, 25.3 ppm). UV-vis absorption spectra were measured with a Varian Cary 50. High Resolution Mass Spectrometry (HRMS-ESI) and Mass Spectrometry (ESI-MS) analyses were performed on a QStar Elite (Applied Biosystems SCIEX) spectrometer or on a SYNAPT G2 HDMS (Waters) spectrometer. These two instruments are equipped with an electrospray ionization source or a matrix-assisted laser desorption/ionization source. Elemental analyses were determined with a Thermo Finnigan EA 1112. The intensity data of the X-ray-quality crystals were collected on a Bruker–Nonius KappaCCD diffractometer using MoKα radiation (λ = 0.71073 Å). Fourier Transform Infrared (FTIR) spectrum was measured with a Bruker VERTEX 70 spectrometer in the Attenuated Total Reflection (ATR) mode using a Pike MIRacle™ ATR accessory.

CCDC-1478912 (**13b**) and CCDC-1478913 (**14**) contain the supplementary crystallographic data. These data can be obtained free of charge from The Cambridge Crystallographic Data Centre via www.ccdc.cam.ac.uk/data_request:cif.

Microscopy: Atomic Force Microscopy technic was performed on a Park XE-100 (Park Systems, Suwon, Korea). AFM image was acquired in tapping-mode, using high-quality probes (HQ-NSC15 by Mikromasch, Sofia, Bulgaria), recorded at a resolution of 512 x 512 pixels and processed with Gwyddion software. Scanning Electron Microscopy (SEM) images were recorded by using a Jeol JSM-6320F operated at 15 kV whereas Transmission Electron Microscopy images were recorded with a Jeol JEM-2010 operated at 200 keV.

DFT calculations: We have used the latest revision of the Gaussian09 program[21] to perform all our computations on **1·2H$^+$, 3b·2H$^+$** and **3c·2H$^+$**, applying default thresholds and algorithms, except when noted below. For all molecules, we have performed geometry optimization of the ground-state structures followed by calculations of the vibrational frequencies, confirming the absence of imaginary frequencies. All structural calculations relied on the PBE0 hybrid exchange-correlation functional,[22] as this parameter-free functional provides accurate geometrical data. We have used the 6-31G(d) atomic basis set for identifying the lowest-energy isomers (see below), and these have been reoptimized with the 6-311G(2d,2p) basis set. The vertical transition energies have been determined with the same functional, namely PBE0, but with a diffuse containing basis set, namely 6-311++G(2d,2p). Next we have computed the NICS[23] at the PBE0/cc-pVTZ level. Environmental effects (methanol) have been systematically accounted for using the well-known Polarizable Continuum Model (PCM) msodel.[24] We have used both the popular linear-response (LR) PCM approach in its non-equilibrium limit.

Organic synthesis: 4,6,16,18-tetranitro-10,12,22,24-tetraamino-2,8,14,20-tetraazacalix[4]arene **4**[1], 10,12,22,24-tetranitro-2,8,14,20-tetraazacalix[4]arene-4,6,16,18-tetra-butyramide **5**,[14] *tert*-butyl 4,6-diamino-1,3-phenylene-*bis*(butylcarbamate) **8a**[15] and 4,6-dinitro-*N*^{1},*N*^{3}-dioctylbenzene-1,3-diamine[25] (precursor of **8b**) were prepared and purified according to literature procedures.

***N*⁴,*N*⁶,*N*¹⁶,*N*¹⁸-tetra*iso*butyl-10,12,22,24-tetranitro-2,8,14,20-tetraaza-calix[4]arene-4,6,16,18-tetraamine 6a:** To a solution of HCl (12N, 20 µL) in THF (v = 100 mL), **4** (m = 50 mg, 82 µmol, 1.0 equiv.) and isobutyraldehyde (60 µL, 0.66 mmol, 8.0 equiv.) were added. The mixture was stirred during 90 min at room temperature, and then cooled to 0 °C before a solution of sodium cyanoborohydride (m = 42 mg, 0.66 mmol, 8.0 equiv.) in THF (v = 2 mL) was added. This mixture was allowed to stir at room temperature for 2.5 hrs and then basified with aqueous NaOH 10%. The solvent was concentrated under reduced pressure and water (v = 15 mL) was added. The aqueous phase was extracted with ethyl acetate and the combined extracts were washed successively with water and brine, dried with $MgSO_4$, and evaporated to dryness. The residue was purified by chromatography on silica gel (cyclohexane/ethyl acetate 2/3, R_f = 0.8) to yield **6a** as a red solid (m = 30 mg, 36 µmol, 44%). ^{1}H NMR (250 MHz, DMSO-d_6): δ 8.99 (s, 2H), 8.85 (br s, 4H), 6.51 (s, 2H), 5.73 (s, 2H), 5.57 (s, 2H), 5.26 (br t, $^3J_{HH}$ = 6.0 Hz, 4H), 2.89-2.69 (m, 8H), 1.85-1.69 (m, 4H), 0.84 (d, $^3J_{HH}$ = 6.6 Hz, 24H). HRMS (ESI-TOF): m/z $[M+H]^+$ for $C_{40}H_{53}N_{12}O_8^+$ calcd. 829.4104, found 829.4110, err. < 1 ppm.

***N*²,*N*⁴,*N*¹⁴,*N*¹⁶-tetra*iso*butyl-azacalixphyrin 3a:** To a suspension of Pd on carbon 5% (m = 20 mg, 9.4 µmol, 32 %mol) in THF (v = 20 mL), **6a** (m = 21 mg, 29.6 µmol, 1.0 equiv.) and hydrazine monohydrate (v = 150 µL, 3.06 mmol, 103 equiv.) were added. The mixture was allowed to heat up to 80 °C for 3 days. After cooling to room temperature, water (v = 20 mL) was added before concentration under reduced pressure. The solid in suspension was then filtered through Celite®, quickly rinsed with water, acetone, diethyl ether and then extracted with methanol. The desired product **3a** was obtained after removing solvent and drying under vacuum as a deep green solid (m = 12.8 mg, 18.2 µmol, 62% yield). M. p. > 300 °C. ^{1}H NMR (400 MHz, MeOD-d_4): δ 6.31 (s, 2H), 5.92 (s, 2H), 3.50 (d, $^3J_{HH}$ = 6.8 Hz, 8H), 2.16-2.09 (m, 4H), 1.05 (d, $^3J_{HH}$ = 6.8 Hz, 24H), -2.75 (s, 2H), -2.91(s, 2H). ^{13}C NMR (100 MHz, MeOD-d_4): δ 161.2, 158.5, 131.3, 130.8, 104.7, 102.5, 94.3, 87.8, 51.8, 29.6, 20.8. HRMS (ESI-TOF): m/z $[M+H]^+$ for $C_{40}H_{55}N_{12}^+$ calcd. 703.4667, found 703.4667, err. < 1 ppm.

***tert*-butyl 4-amino-6-(5-fluoro-2,4-dinitrophenylamino)-1,3-phenylene*bis*(butylcarbamate) 9a** and ***tert*-butyl 4,6-*bis*(5-fluoro-2,4-dinitrophenylamino)-1,3-phenylene*bis*(butylcarbamate) 10a:** To a solution of **8a** (m = 178 mg, 0.395 mmol, 1.0 equiv.) and DFDNB (**7**) (m = 80.6 mg, 0.395 mmol, 1.0 equiv.) in dry MeCN (v = 20 mL), was added N(*i*Pr)$_2$Et (v = 172 µL, 0.987 mmol, 2.5 equiv.). The mixture was stirring under reflux for 3 hrs and the solvent was then removed under reduced pressure. The residue was purified by column chromatography on SiO_2 (ethyl acetate/cyclohexane, 20/80 to 40/60). Evaporation of the solvents under reduced pressure afforded **9a** (m = 45.2 mg, 71.2 µmol) in 18% yield and **10a** (m = 38.1 mg, 46.5 µmol) in 12% yield. Molecule **9a**: ^{1}H NMR (250 MHz, Acetone-d_6): δ 9.91 (br s, 1H), 9.05 (d, $^4J_{HF}$ = 8.0 Hz, 1H), 7.03 (br s, 2H), 6.97 (s, 1H), 4.88 (br s, 2H), 3.73-3.33 (br m, 4H), 1.60-1.16 (m, 26H), 0.91 (t, $^3J_{HH}$ = 7.3 Hz, 3H), 0.76 (t, $^3J_{HH}$ = 7.1 Hz, 3H). ^{13}C NMR (63 MHz, Acetone-d_6): 161.0 (d, $^1J_{CF}$ = 267 Hz), 156.2, 150.0, 149.75, 149.7 (d, $^3J_{CF}$ = 9.0 Hz), 146.5, 135.4, 132.0, 130.0, 129.1, 128.8, 128.6 (d, $^2J_{CF}$ = 9.6 Hz), 114.0, 105.5 (d, $^2J_{CF}$ = 27.7 Hz), 81.9, 81.1, 51.3, 49.4, 32.3, 32.2, 29.5, 29.4, 21.7, 21.5, 15.2, 15.0. HRMS (ESI-TOF): m/z $[M+NH_4]^+$ for $C_{30}H_{47}N_7O_8F^+$ calcd. 652.3465, found 652.3469, err. < 1 ppm. Molecule **10a**: ^{1}H NMR (250 MHz, Acetone-d_6): δ 10.02 (br s, 2H), 9.04 (d, $^4J_{HF}$ = 7.9 Hz, 2H), 7.90 (s, 1H), 7.70 (s, 1H), 7.22 (br d, $^3J_{HF}$ = 13 Hz, 2H), 3.72 (br s, 4H), 1.58-1.14 (m, 26H), 0.78 (t, $^3J_{HH}$ = 7.3 Hz, 6H). ^{13}C NMR (63 MHz, Acetone-d_6): 161.2 (d, $^1J_{CF}$ = 268 Hz), 155.8, 149.6, 149.4, 140.0, 136.4, 130.7, 129.2 (d, $^2J_{CF}$ = 8.8 Hz), 129.0, 126.6, 106.1 (d, $^2J_{CF}$ = 27.7 Hz), 82.9, 51.7, 32.5, 29.4, 21.5, 15.0. HRMS (ESI-TOF): m/z $[M+NH_4]^+$ for $C_{36}H_{48}N_9O_{12}F_2^+$ calcd. 836.3385, found 836.3387, err. < 1 ppm.

***tert*-butyl 4-amino-6-(5-fluoro-2,4-dinitrophenylamino)-1,3-phenylene*bis*(octylcarbamate) 9b** and ***tert*-butyl 4,6-*bis*(5-fluoro-2,4-dinitrophenylamino)-1,3-phenylene*bis*(octylcarbamate) 10b:** To a solution of **8b** (m = 277 mg, 0.492 mmol, 1.0 equiv.) and DFDNB (**7**) (m = 304 mg, 1.49 mmol, 3.0 equiv.) in dry THF (v = 15 mL), 2,4,6-collidine (v = 648 µL, 4.90 mmol, 10 equiv.) was added. The mixture was allowed to heat to reflux for 3 days. The solvent was removed in vacuum. The residue was purified by column chromatography (silica F60, dichloromethane 100), dried in vacuum, giving **9b** in 8% yield (m = 27 mg, 0.0361 mmol) and **10b** in 22% yield (m = 101 mg, 0.108 mmol). Molecule **9b**: ^{1}H NMR (250 MHz, $CDCl_3$): δ 9.87 (br s, 1H), 9.15 (d, $^4J_{HF}$ = 8.0 Hz, 1H), 7.05-6.80 (m, 2H), 6.69 (s, 1H), 3.39-3.37 (br m, 6H), 1.44-1.12 (m, 42H), 0.87-0.80 (m, 6H). ^{13}C NMR (63 MHz, $CDCl_3$): δ 161.5 (d, $^1J_{CF}$ = 267 Hz), 154.4, 147.8, 147.6, 147.5, 143.2, 133.5, 128.9, 128.0, 127.9, 127.5, 126.8, 112.3, 103.6 (d, $^2J_{CF}$ = 27.7 Hz), 81.1, 80.5, 50.3, 48.5, 31.7, 31.6, 29.21, 29.21, 29.13, 29.12, 28.6, 28.6, 28.17, 28.15, 26.72, 26.64, 22.50, 22.45, 13.96, 13.88. HRMS (ESI-TOF): m/z $[M+NH_4]^+$ for $C_{38}H_{63}N_7O_8F^+$ calcd. 764.4717, found 764.4717, err. < 1 ppm. TLC: Silica F60, Ethyl acetate/Cyclohexane 1/2, R_f = 0.45. Molecule **10b**: ^{1}H NMR (250 MHz, $CDCl_3$): δ 9.99 (br s, 2H), 9.11 (d, $^4J_{HF}$ = 7.8 Hz, 2H), 7.44 (s, 1H), 7.38 (s, 1H), 6.93 (d, $^3J_{HF}$ = 12.5 Hz, 2H), 3.80 (br s, 2H), 3.45 (br s, 2H), 1.50-1.11 (m, 42H), 0.84 (d, $^3J_{HH}$ = 6.8 Hz, 6H). ^{13}C NMR (63 MHz, $CDCl_3$): δ 159.6 (d, $^1J_{CF}$ = 267 Hz), 154.1, 147.0, 146.8, 138.1, 134.1, 128.5, 127.6, 127.5 (d, $^2J_{CF}$ = 10.1 Hz), 123.1, 103.5 (d, $^2J_{CF}$ = 27.1 Hz), 82.4, 50.9, 31.6, 29.17, 29.16, 29.02, 28.2, 26.6, 22.5, 13.9. HRMS (ESI-TOF): m/z $[M+NH_4]^+$ for $C_{44}H_{64}N_9O_{12}F_2^+$ calcd. 948.4637, found 948.4636, err. < 1 ppm. TLC: Silica F60, dichloromethane 100, R_f = 0.28

***tert*-butyl 10,12,22,24-tetranitro-2,8,14,20-tetraazacalix[4]arene-4,6,16,18-tetrakis(butylcarbamate) 11a:** To a solution of **8a** (m = 604 mg, 1.34 mmol, 0.42 equiv.) and DFDNB (**7**) (m = 649mg, 3.18 mmol, 1.00 equiv.) in dry MeCN (v = 5 mL), K_2CO_3 (m = 200 mg, 1.45 mmol, 1.1 equiv.) was added. The mixture was allowed to reflux for 24 hrs under stirring. Additional **8a** (m = 716 mg, 1.59 mmol, 0.5 equiv.) was then added and the mixture was further stirred 5 days. The completion of reaction was detected by TLC (ethyl acetate/cyclohexane, 20/80, R_f = 0.25). The resulting product was purified by column chromatography on silica gel (ethyl acetate/cyclohexane, 20/80 to 40/60) to give **11a** as an orange solid (m = 544 mg, 0.442 mmol, 31% yield). ^{1}H NMR (250 MHz, $CDCl_3$): δ 9.77 (br s, 4H), 9.31 (s, 2H), 7.45 (s, 2H), 7.18 (s, 2H), 6.57 (br s, 2H), 3.48 (br s, 8H), 1.41-1.21 (m, 52H), 0.86-0.79 (m, 18H). ^{1}H NMR (250 MHz, Acetone-d_6): δ 9.68 (br s, 4H), 9.16 (s, 2H), 7.78 (br s, 2H), 7.51 (s, 2H), 6.54 (br s, 2H), 3.55 (br s, 8H), 1.39-1.17 (m, 52H), 0.98-0.74 (m, 18H). ^{13}C NMR (63 MHz, $CDCl_3$): δ 153.8, 146.4, 136.9, 135.3, 129.2, 127.5, 125.5, 123.1, 94.2, 81.4, 50.3, 30.9, 28.0, 19.6, 13.4. HRMS (ESI-TOF): m/z $[M+NH_4]^+$ for $C_{60}H_{88}N_{13}O_{16}^+$ calcd. 1246.6467, found 1246.6471, err. < 1 ppm.

***N*²,*N*⁴,*N*¹⁴,*N*¹⁶-tetrabutyl-azacalix[4]phyrin 3b:** To a solution of **11a** (m = 157 mg, 0.128 mmol, 1.0 equiv.) in EtOH (v = 15 mL), $SnCl_2{\cdot}2H_2O$ (m = 577 mg, 2.56 mmol, 20.0 equiv.) and HCl (12N, v = 0.6 mL) were added. The mixture was allowed to reflux overnight. After cooling to room temperature, the solution was carefully neutralized by $NaHCO_3$. Then two spatulas of Celite® were added into the suspension and the solvent was removed under reduced pressure. The residue was taken up into a Soxhlet extractor, rinsed with dichloromethane and extracted with MeOH. After concentration, the desired product **3b** was obtained as a dark green solid (m = 52.4 mg, 0.0745 mmol, 59% yield). M. p. > 300 °C. ^{1}H NMR (250 MHz, DMSO-d_6): δ 8.98 (br s, 4H), 8.64 (br s, 6H), 6.30 (s, 2H), 5.99 (s, 2H), 3.65 (m, 8H), 1.76 (m, 8H), 1.50 (m, $^3J_{HH}$ = 7.2 Hz, 8H), 0.97 (t, $^3J_{HH}$ = 7.2 Hz, 12H), -1.94 (br s, 4H). No ^{13}C NMR spectrum of **3b** could be recorded owing to its poor solubility. HRMS (ESI-TOF): m/z $[M+H]^+$ for $C_{40}H_{55}N_{12}^+$ calcd. 703.4667, found 703.4667, err. < 1 ppm.

***N*¹,*N*⁵-dioctylbenzene-1,2,4,5-tetraamine dihydrochloride 12b:** To a solution of **8b** (m = 303 mg, 0.538 mmol) in dichloromethane (v = 5 mL), HCl (12N, v = 2 mL) was added. This mixture was stirring under argon overnight. The result solid in suspension was collected by a filtration, rinsed with CH_2Cl_2 (v = 20 mL), and dried in vacuum to afford the desired product **12b** (m = 196 mg, 0.449 mmol, 84% yield) as a light pink solid. This crude product was used directly without further purifications. ^{1}H NMR (250 MHz, DMSO-d_6): δ 6.85 (br s, 1H), 6.44 (br s, 1H), 3.06 (t, $^3J_{HH}$ = 7.2 Hz, 4H), 1.62 (m, 4H), 1.35-1.26 (m, 20H), 0.86 (t, $^3J_{HH}$ = 6.8 Hz, 6H). No ^{13}C NMR spectrum could be recorded owing to the poor stability in solution. MALDI-TOF MS: m/z $M^{+\bullet}$ for $C_{22}H_{42}N_4^{\cdot+}$ calcd. 362.3, found 362.3 (100%),

***N*^{1},*N*^{5}-dibutyl-*N*^{2},*N*^{4}-bis(5-fluoro-2,4-dinitrophenyl)benzene-1,2,4,5-tetraamine 13a:** To a solution of *tert*-butyl 4,6-dinitro-1,3-phenylene *bis*(butylcarbamate) **8a** (m = 800 mg, 1.78 mmol) in CH_2Cl_2 (v = 6 mL), HCl (12N, v = 6 mL) was added. This mixture was maintained under argon overnight. The solvent was then removed in vacuum to give a light pink solid **12a** (m = 583 mg, 1.80 mmol, quantitative yield) which was used directly for following step without purification and characterization. To a solution of DFDNB (**7**) (m = 638 mg, 3.12 mmol, 1.8 equiv.) in dry MeCN (100 mL), **12a** (m = 568 mg, 1.76 mmol, 1.0 equiv.) was added. The flask was sealed, cooled down in a water-ice bath and degassed. Degassed N(*i*Pr)$_2$Et (v = 2 mL, 11.6 mmol, 6.6 equiv.) was then added dropwise by a syringe under argon. The solution was stirred at 0 °C for 2 hrs, and at room temperature overnight. After addition of EtOH (v = 100 mL) and cooling in freezer for 4 hrs, the resulting product was collected by a filtration, and rinsed with EtOH (v = 2 x 30 mL), dried under vacuum to afford the desired product **13a** as an orange powder (m = 518 mg, 0.84 mmol, overall yield 54%). ^{1}H NMR (400 MHz, DMSO-d$_6$): δ 9.62 (br s, 2H), 8.90 (d, $^4J_{HF}$ = 8.2 Hz, 2H), 6.84 (s, 1H), 6.50 (d, $^3J_{HF}$ = 14.8 Hz, 2H), 5.97 (s, 1H), 5.54 (br t, $^3J_{HH}$ = 5.5 Hz, 2H), 3.10 (q, $^3J_{HH}$ = 6.4 Hz, 4H), 1.51 (quint, $^3J_{HH}$ = 7.3 Hz, 4H), 1.30 (sext, $^3J_{HH}$ = 7.3 Hz, 4H), 0.88 (t, $^3J_{HH}$ = 7.3 Hz, 6H). ^{13}C NMR (100 MHz, DMSO-d$_6$): δ 158.6 (d, $^1J_{CF}$ = 266 Hz), 150.2, 150.0, 145.1, 128.1, 126.9, 125.2 (d, $^2J_{CF}$ = 9.9 Hz), 109.5, 103.0 (d, $^2J_{CF}$ = 27.3 Hz), 92.0, 41.9, 30.5, 19.7, 13.7. HRMS (ESI-TOF): m/z [M+H]$^+$ for $C_{26}H_{29}N_8O_8F_2^+$ calcd. 619.2071, found 619.2071, err. < 1 ppm.

***N*^{1},*N*^{5}-*bis*(5-fluoro-2,4-dinitrophenyl)-*N*^{2},*N*^{4}-dioctylbenzene-1,2,4,5-tetraamine 13b:** To a solution of DFDNB (**7**) (m = 258 mg, 1.27 mmol, 1.8 equiv.) in MeCN (v = 25 mL) was added **12b** (m = 306 mg, 0.703 mmol, 1.0 equiv.). The flask was closed with a septum and the solution was cooled down in a water-ice bath and degassed. N(*i*Pr)$_2$Et (v = 735 µL, 4.22 mmol, 6.0 equiv.) was then added dropwise by a syringe under argon. The solution was stirring at 0 °C for 2 hrs and to room temperature for additional 2 hrs. The solution was concentrated under vacuum, and the residue was taken up with EtOH (v = 30 mL) and MeCN (v = 10 mL). The obtained solid in suspension was collected by a filtration, rinsed with EtOH (v = 100 mL) and Et$_2$O (v = 20 mL), and dried in vacuum to afford the desired product **13b** as an orange powder (m = 365 mg, 0.499 mmol, 79% yield).^{1}H NMR (250 MHz, $CDCl_3$): δ 9.29 (br s, 2H), 9.15 (d, $^4J_{HF}$ = 7.8 Hz, 2H), 6.84 (s, 1H), 6.52 (d, $^3J_{HF}$ = 13 Hz, 2H), 6.07 (s, 1H), 3.97 (br s, 2H), 3.19 (t, $^3J_{HH}$ = 7.0 Hz, 4H), 1.66-1.26 (m, 24H), 0.88 (t, $^3J_{HH}$ = 7.0 Hz, 6H). ^{1}H NMR (250 MHz, Acetone-d$_6$): δ 9.60 (br s, 2H), 9.01 (d, $^4J_{HF}$ = 8.0 Hz, 2H), 7.08 (s, 1H), 6.70 (d, $^3J_{HH}$ = 14.3 Hz, 2H), 6.20 (s, 1H), 5.13 (br s, 2H), 3.24 (t, $^3J_{HH}$ = 7.0 Hz, 4H), 1.66-1.55 (m, 4H), 1.29-1.26 (m, 20H), 0.87 (t, $^3J_{HH}$ = 7.0 Hz, 6H). ^{13}C NMR (63 MHz, $CDCl_3$): δ 159.9 (d, $^1J_{CF}$ = 267 Hz), 150.0, 149.8, 146.1, 127.9, 127.6, 127.3 (d, $^2J_{CF}$ = 10.1 Hz), 109.8, 103.7 (d, $^2J_{CF}$ = 27.7 Hz), 93.4, 43.5, 31.7, 29.28, 29.23, 29.18, 27.1, 22.6, 14.0. HRMS (ESI-TOF): m/z [M+H]$^+$ for $C_{34}H_{45}N_8O_8F_2^+$ calcd. 731.3323, found 731.3323, err. < 1 ppm. TLC: Silica F60, dichloromethane/cyclohexane 70/30, R_f = 0.34.

***N*^{1},*N*^{2},*N*^{4}-*tris*(5-fluoro-2,4-dinitrophenyl)-*N*^{1},*N*^{5}-dioctylbenzene-1,2,4,5-tetraamine 14:** To a solution of DFDNB (**7**) (m = 315 mg, 1.54 mmol, 2.23 equiv.) in anhydrous MeCN (v = 20 mL), **12b** (m = 300 mg, 0.689 mmol, 1.0 equiv.) was added. The flask was closed by a septum. The system was degassed and N(*i*Pr)$_2$Et (v = 1.0 mL, 5.74 mmol, 8.3 equiv.) was added dropwise by a syringe under argon. The solution was allowed to warm to room temperature for 3 days and finally heated up to reflux for 2 hrs. The solvent was removed by reducing pressure. The residue was purified by column chromatography (silica F60, DCM/cyclohexane, 70/30 to 90/10) to afford the major product **13b** (m = 142.7 mg, 0.195 mmol, 29% yield) and the product **14** (m = 33.9 mg, 0.081 mmol, 12% yield). ^{1}H NMR (250 MHz, $CDCl_3$): δ 9.67 (br, 1H), 9.42 (br s, 1H), 9.13 (d, $^4J_{HF}$ = 7.6 Hz, 1H), 9.10 (d, $^4J_{HF}$ = 7.7 Hz, 1H), 8.48 (d, $^4J_{HF}$ = 7.7 Hz, 1H), 7.24 (s, 1H), 6.98 (d, $^3J_{HF}$ = 13.1 Hz, 1H), 6.83 (d, $^3J_{HF}$ = 12.7 Hz, 1H), 6.43 (d, $^3J_{HF}$ = 12.7 Hz, 1H), 6.30 (s, 1H), 4.25 (br t, $^3J_{HH}$ = 5.4 Hz, 1H), 3.60 (t, $^3J_{HH}$ = 7.8 Hz, 2H), 3.05 (td, $^3J_{HH}$ = 6.7 Hz, $^3J_{HH}$ = 5.8 Hz, 2H), 1.73-1.49 (m, 4H), 1.23-1.20 (m, 20H), 0.87-0.82 (m, 6H). ^{1}H NMR (400 MHz, DMSO-d$_6$): δ 9.85 (br s, 1H), 9.54 (br s, 1H), 8.93 (d, $^4J_{HF}$ = 8.0 Hz, 1H), 8.90 (d, $^4J_{HF}$ = 8.0 Hz, 1H), 8.53 (d, $^4J_{HF}$ = 8.0 Hz, 1H), 7.57 (d, $^3J_{HF}$ = 14.3 Hz, 1H), 7.27 (s, 1H), 7.08 (d, $^3J_{HF}$ = 13.8 Hz, 1H), 6.40 (s, 1H), 6.30 (d, $^3J_{HF}$ = 14.0 Hz, 1H), 6.05 (br t, $^3J_{HH}$ = 5.8 Hz, 1H), 3.69 (t, $^3J_{HH}$ = 7.5 Hz, 2H), 2.96 (td, $^3J_{HH}$ = 6.5 Hz, $^3J_{HH}$ = 6.3 Hz, 2H), 1.60 (quint, $^3J_{HH}$ = 7.4 Hz, 2H), 1.35 (quint, $^3J_{HH}$ = 6.3 Hz, 2H), 1.25-1.11 (m, 20H), 0.85-0.79 (m, 6H). ^{13}C NMR (100 MHz, DMSO-d$_6$): δ 158.9 (d, $^1J_{CF}$ = 267 Hz), 158.6 (d, $^1J_{CF}$ = 266 Hz), 157.5 (d, $^1J_{CF}$ = 267 Hz), 154.1, 148.6, 148.5, 147.66, 147.52, 147.21, 147.05, 144.7, 141.9, 135.6, 128.7, 128.2, 127.8, 127.15, 127.02, 126.7, 126.48, 126.38, 125.8, 125.7, 120.5, 118.7, 108.5 (d, $^2J_{CF}$ = 27.0 Hz), 108.2, 103.4 (d, $^2J_{CF}$ = 26.0 Hz), 103.1 (d, $^2J_{CF}$ = 28.0 Hz), 53.2, 41.7, 31.15, 31.12, 28.8, 28.63, 28.55, 28.50, 28.2, 26.7, 26.4, 25.9, 21.96, 21.92, 13.8, 13.8. HRMS (ESI-TOF): m/z [M+NH$_4$]$^+$ for $C_{40}H_{49}N_{11}O_{12}F_3^+$ calcd. 932.3509 found 932.3509, err. < 1 ppm. TLC: Silica F60, dichloromethane 100, R_f = 0.58.

***N*^{4},*N*^{6}-dibutyl-10,12,22,24-tetranitro-2,8,14,20-tetraazacalix[4]arene-4,6,16,18-tetraamine 6c:** To a solution of **13a** (m = 200 mg, 0.323 mmol, 1.0 equiv.) in anhydrous MeCN (v = 80 mL), TAB·4HCl (**12c**) (m = 101 mg, 0.355 mmol, 1.1 equiv.) was added. The flask was sealed, degassed and N(*i*Pr)$_2$Et (v = 495 µL, 2.84 mmol, 8.0 equiv.) was added dropwise by a syringe under argon. The mixture was allowed to sonicate for 1 hr, maintain at room temperature for additionally 2 hrs under stirring, and finally under reflux overnight. After concentration of the solvent under vacuum, the residue was rinsed with a mixture of MeCN (v = 10 mL) and EtOH (v = 40 mL), isolated by filtration, washed with EtOH (v = 3 x 20 mL), and dried under vacuum to afford the desired product **6c** as a brown powder (m = 191 mg, 0.266 mmol, 83% yield). ^{1}H NMR (400 MHz, THF-d$_8$): δ 9.12 (s, 2H), 9.00 (br s, 4H), 6.60 (s, 1H), 6.53 (s, 1H), 6.05 (s, 1H), 5.90 (s, 1H), 5.63 (s, 2H), 4.66 (br t, $^3J_{HH}$ = 5.2 Hz, 2H), 4.48 (br s, 4H), 3.10 (q, $^3J_{HH}$ = 6.8 Hz, 4H), 1.54 (m, 4H), 1.38 (sext, $^3J_{HH}$ = 7.2 Hz, 4H), 0.94 (t, $^3J_{HH}$ = 7.2 Hz, 6H). ^{13}C NMR (100 MHz, THF-d$_8$): δ 150.69, 150.68, 147.3, 147.0, 130.6, 130.2, 128.5, 126.0, 125.9, 133.3, 112.0, 100.8, 96.5, 93.4, 44.0, 32.3, 21.2, 14.4. HRMS (ESI-TOF): m/z [M+H]$^+$ for $C_{32}H_{37}N_{12}O_8^+$ calcd. 717.2852, found 717.2852, err. < 1 ppm.

***N*^{4},*N*^{6}-dioctyl-10,12,22,24-tetranitro-2,8,14,20-tetraazacalix[4]arene-4,6,16,18-tetraamine 6d:** To a solution of **13b** (m = 80 mg, 0.109 mmol, 1.0 equiv.) in dry MeCN (v = 10 mL), TAB·4HCl (**12c**) (m = 32.4 mg, 0.114 mmol, 1.05 equiv.) was added. The flask was closed by a septum, and cooled in a water-ice bath. The system was degassed and N(*i*Pr)$_2$Et (v = 159 µL, 912 mmol, 8.4 equiv.) was added dropwise by a syringe under argon. The solution was allowed to sonicate at room temperature for 40 min, and then heated to reflux overnight. After cooling down to room temperature, the obtained solid in suspension was collected by a filtration, rinsed with EtOH (v = 100 mL), Et$_2$O (v = 10 mL), and dried in vacuum to afford the desired product **6d** (m = 63.2 mg, 0.076 mmol, 70% yield) as a brown powder. ^{1}H NMR (250 MHz, Acetone-d$_6$): δ 9.10 (s, 2H), 8.97 (br s, 4H), 6.70 (s, 1H), 6.66 (s, 1H), 6.27 (s, 1H), 5.99 (s, 1H), 5.76 (s, 2H), 4.91 (br t, $^3J_{HH}$ = 5.7 Hz, 2H), 4.70 (br s, 4H), 3.15 (td, $^3J_{HH}$ = 7.0 Hz, $^3J_{HH}$ = 5.7 Hz, 4H), 1.65-1.50 (m, 4H), 1.41-1.20 (m, 20H), 0.87 (t, $^3J_{HH}$ = 7.0 Hz, 6H). ^{13}C NMR (63 MHz, Acetone-d$_6$): δ 151.77, 151.75, 148.4, 148.0, 131.5, 131.1, 129.7, 127.1, 127.0, 114.0, 112.5, 102.4, 97.3, 94.6, 45.2, 33.6, 31.4, 31.2, 30.9, 29.0, 24.4, 15.4. HRMS (ESI-TOF): m/z [M+H]$^+$ for $C_{40}H_{53}N_{12}O_8^+$ calcd. 829.4104, found 829.4106, err. < 1 ppm.

***N*^{4},*N*^{6},*N*^{16},*N*^{18}-tetraoctyl-10,12,22,24-tetranitro-2,8,14,20-tetraazacalix[4]-arene-4,6,16,18-tetraamine 6e:** To a solution of **13b** (m = 160 mg, 0.219 mmol, 1.0 equiv.) in dry MeCN (v = 30 mL), **12b** (m = 115 mg, 0.263 mmol, 1.2 equiv.) was added. The flask was sealed, degassed and N(*i*Pr)$_2$Et was added dropwise (m = 370 µL, 2.12 mmol, 9.6 equiv.) by a syringe under argon. The mixture was allowed at room temperature for 2 hrs under stirring, and then heated to reflux overnight. After concentration the solvent under vacuum, the residue was taken up with a mixture of acetone (v = 5 mL) and ethanol (v = 5 mL). The resulting solid was isolated by filtration, washed with EtOH, and dried under vacuum to afford the desired product **6e** (m = 155.5 mg, 0.148 mmol, 68% yield) as an orange powder. ^{1}H NMR (250 MHz, $CDCl_3$): δ 9.26 (s, 2H), 8.85 (br s, 4H), 6.58 (s, 2H), 5.82 (s, 2H), 5.49 (s, 2H), 3.91 (br t, $^3J_{HH}$ = 5.4 Hz, 4H), 3.09-2.99 (m, 8H), 1.53-1.28 (m, 48H), 0.89 (t, $^3J_{HH}$ = 6.8 Hz, 12H). ^{13}C NMR (63 MHz, $CDCl_3$): δ 149.9, 146.4, 129.2, 129.0, 125.4, 110.6, 95.7, 92.6, 43.8, 31.8, 29.49, 29.46, 29.33, 27.3, 22.7, 14.1. HRMS (ESI-TOF): m/z [M+H]$^+$ for $C_{56}H_{85}N_{12}O_8^+$ calcd. 1053.6608, found 1053.6608, err. < 1 ppm. TLC: Silica F60, dichloromethane/ cyclohexane 70/30, R_f = 0.29

***N*²,*N*⁴-dibutyl-azacalixphyrin 3c:** To a mixture of **6c** (m = 50 mg, 69.8 µmol) and $SnCl_2{\cdot}2H_2O$ (m = 500 mg, 2.22 mmol, 32 equiv.) in a pressure bomb, HCl (12N, v = 5 mL) was added. The pressure bomb was closed by a Teflon® seal, and allowed to warm at 40 °C overnight. The resulting solid in suspension was collected by filtration, rinsed with HCl (12N, v = 2 x 5 mL) and Et_2O (v = 10 mL) to give a pink-pale powder, and then dissolved in hot water (v = 100 mL). This solution was neutralized carefully with dropping an aqueous solution of NaOH (10% w/w), until the pH value reached nearly 7-8. The solution was then stirred and exposed under air for 3 hrs. The obtained precipitate was isolated by filtration, washed with DMSO (v = 2 x 3 mL), acetone, and dried in vacuum to afford a desired product **3c** as a dark green solid (m = 34 mg, 57.6 µmol, 83% yield). M. p > 300 °C. ^{1}H NMR (400 MHz, DMSO-d_6): δ 9.03 (br s, 2H), 8.59 (br s, 10H), 6.28 (s, 3H), 5.99 (s, 1H), 3.65 (m, 4H), 1.75 (quint, $^3J_{HH}$ = 7.2 Hz, 4H), 1.44 (sext, $^3J_{HH}$ = 7.2 Hz, 4H), 0.96 (t, $^3J_{HH}$ = 7.2 Hz, 6H), -1.86 (br s, 4H). No ^{13}C NMR spectrum of **3c** could be recorded owing to its poor solubility. HRMS (ESI-TOF): m/z $[M+H]^+$ for $C_{32}H_{37}N_{12}O_8^+$ calcd. 591.3415, found 591.3421, err. < 2 ppm.

***N*²,*N*⁴-dioctyl-azacalixphyrin 3d:** Molecule **6d** (m = 30.5 mg, 36.8 µmol) and Pd on carbon 5% (m = 1.6 mg, 0.75 µmol, 5 %mol) was put into a pressure bomb. Then THF (v = 10 mL) and hydrazine monohydrate (v = 50 µL, 1.02 mmol) was added. The pressure bomb was closed by a Teflon® seal, and allowed to heat at 80 °C for 4 days. The mixture was then put into MeOH (v = 50 mL), and stirred under air at room temperature for 24 hrs. Pd/C was removed then by filtration on Celite®. After removal of the solvents under vacuum, the desired product **3d** was obtained as a dark green solid (m = 14 mg, 20.0 µmol, 55% yield). M. p. > 300 °C. ^{1}H NMR (400 MHz, DMSO-d_6): δ 9.10 (br s, 2H), 8.56 (br s, 10H), 6.31 (s, 3H), 5.96 (s, 1H), 3.71-3.53 (m, 4H), 1.81-167 (m, 4H), 1.38-1.06 (m, 20H), 0.83-0.75 (m, 6H), -1.96 (br s, 4H). No ^{13}C NMR spectrum of **3d** could be recorded owing to its poor solubility. HRMS (ESI-TOF): m/z $[M+H]^+$ for $C_{40}H_{55}N_{12}^+$calcd. 703.4667, found 703.4667, err. < 1 ppm.

***N*²,*N*⁴,*N*¹⁴,*N*¹⁶-tetraoctyl-azacalixphyrin 3e: 6e** (m = 51.2 mg, 48.6 µmol) and Pd on carbon 5% (m = 28 mg, 13.2 µmol, 27 %mol) were placed into a pressure bomb. Then, THF (v = 25 mL) and hydrazine monohydrate (v = 300 µL, 6.11 mmol) were added. The pressure bomb was closed by a Teflon® seal, and allowed to heat up to 80 °C for 2 days. After concentration under reduced pressure, MeOH (v = 30 mL) was added and the solution was stirred under air at room temperature for 24 hrs. Pd/C was then removed by filtration on Celite®. After removal of the solvents under vacuum, the desired product **3e** was obtained as a dark green solid (m = 39.8 mg, 42.9 µmol, 89% yield). M. p. > 300 °C. ^{1}H NMR (250 MHz, MeOD-d_4): δ 6.23 (s, 2H), 5.82 (s, 2H), 3.71-3.66 (m, 8H), 1.99-1.93 (m, 8H), 1.58-1.32 (m, 40H), 0.89 (t, $^3J_{HH}$ = 6.8 Hz, 12H), -3.34 (s, 2H), -3.45 (s, 2H). ^{13}C NMR (63 MHz, MeOD-d_4): δ 161.0, 157.9, 130.6, 129.9, 103.5, 102.3, 94.4, 87.6, 44.9, 33.1, 30.8, 30.6, 30.0, 28.6, 23.8, 14.5. HRMS (ESI-TOF): m/z $[M+2H]^{2+}$ for $C_{56}H_{88}N_{12}^{2+}$ calcd. 464.3622, found 464.3620, err. < 1 ppm

Acknowledgements

D.J. and O.S. thank the ANR for financial support in the framework of the EMA project. G.M. thanks the *Région des Pays de la Loire* for his postdoctoral grant in the framework of the SAPOMAP project. D.J. acknowledges the European Research Council (ERC) and the *Région des Pays de la Loire* for financial support in the framework of a Starting Grant (Marches-278845) and the SAPOMAP project, respectively. This research used resources of the GENCI-CINES/IDRIS (Grant c2013085117), CCIPL (Centre de Calcul Intensif des Pays de Loire), and a local Troy cluster.

Keywords: Azacalixarenes • Azacalixphyrines • Ribbon • Aromaticity • Macrocycles

[1] a) Z. Chen, M. Giorgi, D. Jacquemin, M. Elhabiri, O. Siri, *Angew. Chem. Int. Ed.* **2013**, *125*, 6370. b) G. Marchand, A. Laurent, Z. Chen, O. Siri, D. Jacquemin, *J. Phys. Chem. A*, **2014**, *118*, 8883.

[2] a) *Phthalocyanine Molecular Materials, Structure & Bonding* (Ed.: J. Jianzhuang), Springer, Berlin, 2010; b) R. Wu, A. Cetin, W. S. Durfee, C. J. Ziegler, *Angew. Chem.* **2006**, *118*, 5798; *Angew. Chem. Int. Ed*. **2006**, *45*, 5670; c) A. Çetin, W. S. Durfee, C. J. Ziegler, *Inorg. Chem.* **2007**, *46*, 6239; d) S. Sripothongnak, A. M. Pischera, M. P. Espe, W. S. Durfee, C. J. Ziegler, *Inorg. Chem.* **2009**, *48*, 1293; e) S. Sripothongnak, N. Barone, C. J. Ziegler, *Chem. Commun*. **2009**, 4584; f) A. Çetin, S. Sripothongnak, M. Kawa, W. S. Durfee, C. J. Ziegler, *Chem. Commun*. **2007**, 4289.

[3] K. M. Kadish, K. M. Smith, R. Guilard Ed., *Handbook of Porphyrin Science: With Applications to Chemistry, Physics, Materials Science, Engineering, Biology and Medicine*, (World Scientific Press, 2011.

[4] M. Vinodh, F. H. Alipour, A. A. Mohamod, T. F. Al-Azemi, F. Talal, *Molecules* **2012**, *17*, 11763.

[5] L. L. Li, E. W.-G. Diau, *Chem. Soc. Rev.* **2013**, *42*, 291.

[6] W.-D. Jang, Y.-H. Jeong, *Supramolecular Chem.* **2013**, *25*, 34.

[7] H. Yaku, T. Murashima, D. Miyoshi, N. Sugimoto, *Molecules* **2012**, *17*, 10586.

[8] V. Bulach, F. Sguerra, M. W. Hosseini *Coord. Chem. Rev.* **2013**, *256*, 1468.

[9] M. J.Griffith, K. Sunahara, P. Wagner, K. Wagner, G. G. Wallace, D. L. Officer, A. Furube, R. Katoh, S. Mori, A. J. Mozer, *Chem. Commun.* **2012**, *48*, 4145.

[10] H. Fischer, W. Gleim, *Liebigs Ann.* **1936**, *521*, 157.

[11] a) P. Rothemund *J. Am. Chem. Soc.* **1936**, 58, 625. b) M. O. Senge, J. Richter *J. Porphyrins Phthalocyanines* **2004**, *8,* 934.

[12] a) G. Qian, Z. Y. Wang, *Chem. Asian J.* **2010**, *5*, 1006. b) H. Jiang, *Macromol. Rapid Commun*. **2010**, *31*, 2007.

[13] a) N. Koch, Ed., in *Supramolecular Materials for Opto-Electronics* (RSC Press), 2014. b) D. G. Reuven, H. B. M. Shashikala, S. Mandal, M. N. V. Williams, J. Chaudharya, X.-Q. Wang *J. Mater. Chem. B*, **2013**,*1*, 3926. c) A. Nduwimana, X.-Q. Wang *ACS Nano*., **2009**, *3*, 1995. d) P. Samori, F. Cacialli, Ed., in Functional Supramolecular Architectures: For Organic Electronics and Nanotechnology (Wiley-VCH Press), 2014. e) A. Gourdon, Ed., in *On-Surface Synthesis* (Springer Press), 2016.

[14] G. Canard, J. Andeme Edzang, Z. Chen, M. Chessé, M. Elhabiri, M. Giorgi, O. Siri *Chem. Eur. J.* **2016**, *22*, 5756.

[15] C. Seillan, O. Siri, O. *Tetrahedron Lett.* **2009**, *50,* 630.

[16] M. Touil, M. Lachkar, O. Siri, *Tetrahedron Lett.* **2008**, *49,* 7250.

[17] R. Haddoub, M. Touil, J. M. Raimundo, O. Siri, O. *Org. Lett.* **2010**, *12,* 2722.

[18] G. Marchand, P. Giraudeau, Z. Chen, M. Elhabiri, O. Siri, D. Jacquemin *Phys. Chem. Chem. Phys*. **2016**, *18*, 9608.

[19] G. Socrates, Ed., in *Infrared and Raman Characteristic Group Frequencies Third Edition*, (Wiley), 2001.

[20] J. J. Fripiat, M. Pennequin, G. Poncelet, P. Cloos *Clay Minerals* **1969**, *8*, 119.

[21] M. J. Frisch, G. W. Trucks, H. B. Schlegel, G. E. Scuseria, M. A. Robb, J. R. Cheeseman, G. Scalmani, V. Barone, B. Mennucci, G. A. Peters- son, H. Nakatsuji, M. Caricato, X. Li, H. P. Hratchian, A. F. Izmaylov, J. Bloino, G. Zheng, J. L. Sonnenberg, M. Hada, M. Ehara, K. Toyota, R. Fukuda, J. Hasegawa, M. Ishida, T. Nakajima, Y. Honda, O. Kitao, H. Nakai, T. Vreven, J. A. Montgomery, Jr., J. E. Peralta, F. Ogliaro, M. Bearpark, J. J. Heyd, E. Brothers, K. N. Kudin, V. N. Staroverov, R. Kobayashi, J. Normand, K. Raghavachari, A. Rendell, J. C. Burant, S. S. Iyengar, J. Tomasi, M. Cossi, N. Rega, J. M. Millam, M. Klene, J. E. Knox, J. B. Cross, V. Bakken, C. Adamo, J. Jaramillo, R. Gomperts, R. E. Stratmann, O. Yazyev, A. J. Austin, R. Cammi, C.

Pomelli, J. W. Ochterski, R. L. Martin, K. Morokuma, V. G. Zakrzewski, G. A. Voth, P. Salvador, J. J. Dannenberg, S. Dapprich, A. D. Daniels, O. Farkas, J. B. Foresman, J. V. Ortiz, J. Cioslowski and D. J. Fox, *Gaussian 09 Revision D.01*, 2009, Gaussian Inc. Wallingford CT.

[22] C. Adamo, V. Barone, *J. Chem. Phys.* **1999**, *110,* 6158.

[23] Z. Chen, C. S. Wannere, C. Corminboeuf, R. Puchta, P. von Ragué Schleyer, *Chem. Rev.* **2005**, *105*, 3842.

[24] J. Tomasi, B. Mennucci and R. Cammi, *Chem. Rev.*, **2005**, *105*, 2999.

[25] H. S. Nalwa, T. Watanabe, K. Ogino, H. Sato, S. Miyata, *J. Mater. Sci.* **1998**, *33*, 3699.